

A coupled FEM-BEM approach for crack growth simulation under fatigue load spectrum

C. Calì, R. Citarella, G. Cricri, M. Perrella

University of Salerno, Dept. of Mechanical Engineering, Fisciano (SA), Italy,
rcitarella@unisa.it

ABSTRACT. *This paper describes an original implementation of a two-parameters crack growth model for 2D crack propagation simulations under general load spectrum. In such model, in order to unify the damage process, the following basic parameters are introduced for describing the overall fatigue process: ΔK , K_{max} and the internal stress contribution to K_{max} .*

The coupled usage of Finite Element Method (FEM) and Dual Boundary Element Method (DBEM) is proposed in order to take advantage of the main capabilities of the two methods. The procedure is validated by comparison with in house obtained experimental results and its capability to predict the retardation phenomena following an overload is assessed. The numerical procedure is tested with reference to an MT aluminium specimen (2024HP-T3), whose fatigue calibration parameters had been previously determined using a CT specimen undergoing a constant amplitude load. As a matter of fact the main advantage of the aforementioned procedure is based on the simplicity of the crack growth law calibration, in fact, there is no need to calibrate on various overload levels but few constant amplitude test are sufficient.

One of the main capabilities of the implemented procedure is the possibility to simulate load spectrum effects under linear elastic fracture mechanics, being the plastic effects simulated by ad hoc body loads, imposed in the BEM analysis (by means of “load lines”), without the need for any non physical calibration parameters, as in many phenomenological models aimed at load spectra allowance (Willenborg model, Wheeler model, etc.). A curvilinear crack path is simulated and reproduced experimentally: the differences between the calculated and experimental delay cycles after an overload are comparable with the typical scatter of such kind of test.

INTRODUCTION

In this work, the implementation of a two-parameters crack growth model [1-2], is recalled [3] and its application to a propagation problem with a curvilinear crack path is described in details.

The coupled usage of finite element method (FEM) and dual boundary element method (DBEM) is proposed in order to take advantage of the main capabilities of the two methods: FEM is more efficient for elastic-plastic analysis (needed to asses the residual

stress profile) whilst BEM allows an efficient automatic crack propagation, especially for complex geometry or for mixed mode conditions.

In particular, the Dual Boundary Element Method (DBEM), as implemented in the commercial code BEASY, is adopted for the crack propagation simulation [4] whilst the FEM code ANSYS is used to calculate the residual stresses by elastic-plastic analysis.

The proposed application is based on a series of laboratory tests, realised in order to evaluate the capabilities of the implemented procedure in predicting the crack retardation phenomena induced by an overload.

FATIGUE TEST AND SCATTER ASSESSMENT (MT SPECIMEN)

Considering the experimental scatter inherent in the crack retardation phenomena (the considered specimens are thin and the delay cycles scatter increases along with thickness reduction), a consistent number of specimens is to be fatigue cycled under the same nominal conditions in order to assess the material stochastic behaviour [5]. The eight MT specimens tested are rectangular plate with a central hole of diameter $d=5$ mm and thickness 2.8 mm, fatigue loaded with a predefined spectra using an INSTRON 8502 machine (Fig. 1). The material is 2024HP-T3 clad sheet and the tested specimens has the following geometric dimensions and mechanical properties:

- width $W=70$ mm, length $L=300$ mm, thickness $t=2.8$ mm, hole diameter $\phi=5$ mm;
- Young modulus $E=72$ GPa, Poisson coefficient $\nu=0.3$.

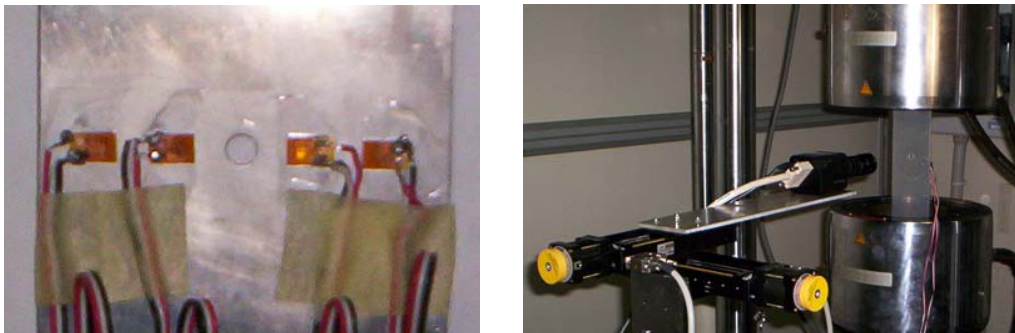


Figure 1. Strain gauge configuration and motorised optical monitoring system.

When an initial crack is devised, by an automatic strain gauge monitoring system, the monitoring of the propagation phase, by a motorised vision system, can start. In particular the fatigue load is stopped when one of the two events, crack gauge breaking or strain gauge signal variation superior to a predefined threshold, is verified, whilst the digital camera is automatically moved in order to remain focused on the moving crack tip [6]. Once the crack is initiated a load spectra is applied, consisting of a constant amplitude baseline load with intermingled overloads of variable intensity ($R_{OL}=1.4-2$).

The spectrum load applied, with a frequency of 10 Hz, for the crack initiation and propagation is described in Table 1.

Table 1. Spectrum load applied to specimens N. 1-8.

| | Initiation load | First overload (+100%) | Baseline fatigue load | Second overload (+50%) | Baseline fatigue load | Third overload (+40%) | Baseline fatigue load |
|---------------------|-----------------|------------------------|-----------------------|------------------------|-----------------------|-----------------------|-----------------------|
| P_{max} [kN] | 18.00 | 36.00 | 18.00 | 27 | 18.00 | 25.2 | 18.00 |
| P_{min} [kN] | 0.90 | 0.90 | 0.90 | 0.9 | 0.90 | 0.9 | 0.90 |
| $R=P_{min}/P_{max}$ | 0.05 | 0.025 | 0.05 | 0.033 | 0.05 | 0.036 | 0.05 |

The crack initiation time is highly scattered, probably as a consequence of a non uniform drilling process and in general of a non standardised and controlled plate manufacturing process. In Fig. 2 a graph plot is reported with reference crack behaviour after the first overload (100%): in this first part of the propagation only the data from three specimens (N. 1, 6 and 8) were available even if few more specimen would be necessary for an appropriate statistical treatment (the points considered for the delay cycles assessment are enlarged).

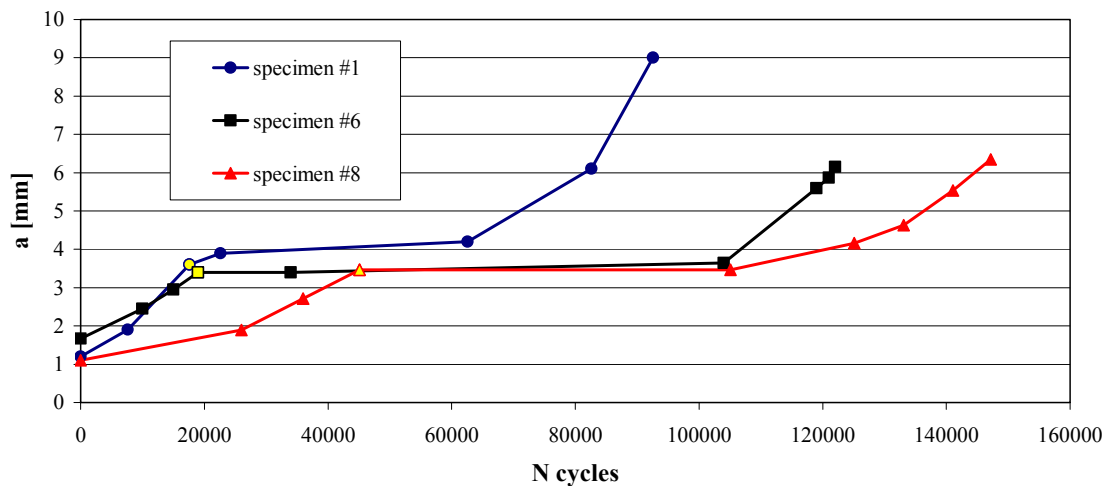


Figure 2. Crack length vs. cycles, after the first overload, for the specimens N. 1, 6, 8.

Anyway in Table 2 the corresponding mean value and standard deviation of delay cycles are reported (the delay phenomena is considered ending when the propagating crack reach again the same crack growth rate as immediately before the overload application).

After complete recovery from the transient behaviour associated to the first overload, (with a reached crack length of about 6 mm for the specimen N. 6) a second 50% overload (one cycle) is applied (Table 1).

Table 2. Scatter assessment of delay time after 100% overload.

| | 100% overload application | End of delay | Delay cycles |
|---------------------------------------|---------------------------|--------------|--------------|
| Specimen 1 | 17606 | 62606 | 45000 |
| Specimen 2 | 19001 | 104001 | 85000 |
| Specimen 3 | 45101 | 125101 | 80000 |
| Delay cycles mean value | | | 70000 |
| Delay cycles standard deviation | | | 21794 |
| Delay cycles coefficient of variation | | | 31.1 % |

The propagation data related to the second 50 % overload and to the specimens N. 4-7 are shown in Fig. 3. This time the data from four specimen are available for statistical regression (Table 3).

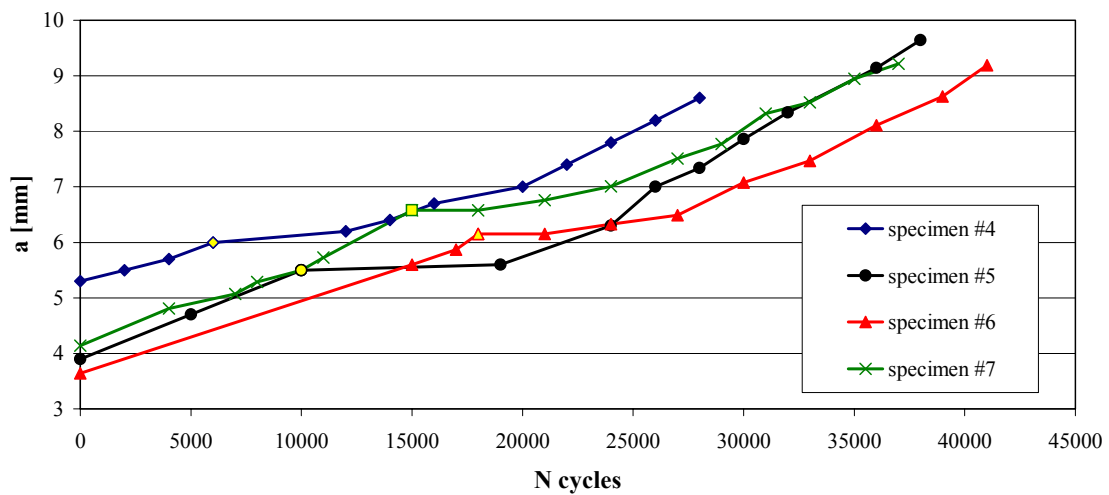


Figure 3. Crack length vs. cycles for the specimens N. 4-7 after the second overload.

Table 3. Scatter assessment of delay time.

| | 50% overload application at cycles: | End of delay at cycles: | Delay cycles |
|---------------------------------------|-------------------------------------|-------------------------|--------------|
| Specimen 4 | 6001 | 12001 | 6000 |
| Specimen 5 | 10001 | 19001 | 9000 |
| Specimen 6 | 18001 | 27001 | 9000 |
| Specimen 7 | 15001 | 24001 | 9000 |
| Delay cycles mean value | | | 8250 |
| Delay cycles standard deviation | | | 1500 |
| Delay cycles coefficient of variation | | | 18.1 % |

After complete recovery from the transient behaviour associated to the second overload, a third 40% overload was applied for one cycle (Table 1) when the crack length is about 11.5 mm. The propagation data related to specimen N. 4-7 are shown in Fig. 4. Again the data from four specimen are available for statistical regression (Table 4).

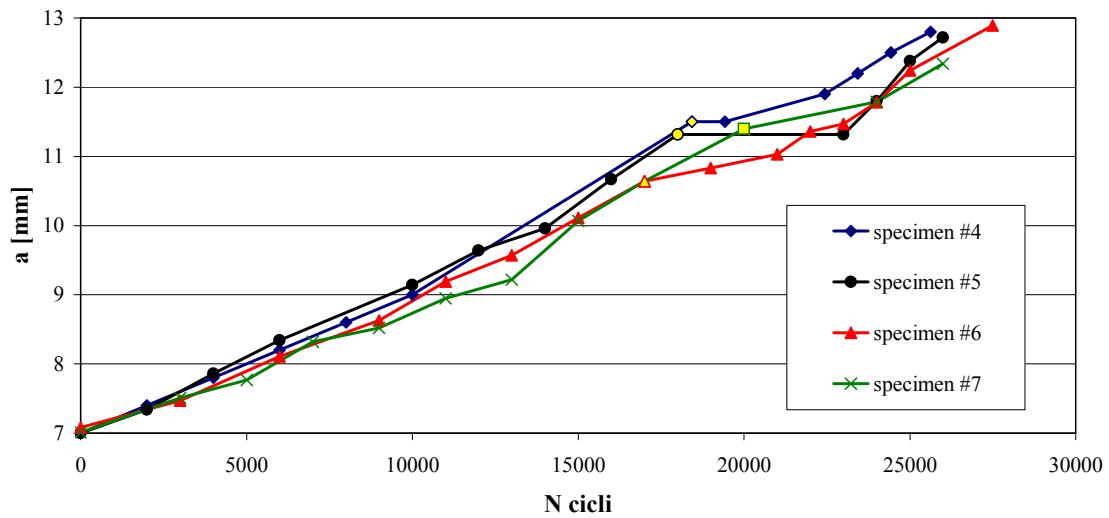


Figure 4. Crack length vs. cycles for the specimens N. 4-7.

Table 4. Scatter assessment of delay time.

| | 50% overload application at cycles: | End of delay at cycles: | Delay cycles |
|---------------------------------------|-------------------------------------|-------------------------|--------------|
| Specimen 4 | 18431 | 22431 | 4000 |
| Specimen 5 | 18001 | 23001 | 5000 |
| Specimen 6 | 17001 | 21001 | 4000 |
| Specimen 7 | 20001 | 24001 | 4000 |
| Delay cycles mean value | | | 4250 |
| Delay cycles standard deviation | | | 500 |
| Delay cycles coefficient of variation | | | 11.7 % |

EXPERIMENTAL-NUMERICAL CORRELATION FOR A CURVILINEAR CRACK PATH (TWO HOLE SPECIMEN)

Having established the experimental data scatter it is possible to assess the accuracy of the numerical results by comparison with the experimental delay cycles from a fatigue test on a complex geometry specimen undergoing a load spectrum (Table 5).

Table 5. Load spectrum description.

| | Load 1 | Load 2 | Load 3 | overload +50% | Load 3 | overload +40% | Load 3 | overload +70% | Load 3 |
|----------------|--------|--------|--------|---------------|--------|---------------|--------|---------------|--------|
| P_{max} [kN] | 18.00 | 14.00 | 16.00 | 24 | 16.00 | 22.4 | 16.00 | 27.2 | 16.00 |
| P_{min} [kN] | 0.90 | 2.10 | 2.40 | 2.4 | 2.40 | 2.4 | 2.40 | 2.4 | 2.40 |
| R | 0.05 | 0.15 | 0.15 | 0.100 | 0.15 | 0.107 | 0.15 | 0.088 | 0.15 |

The specimen has two hole in order to induce a curved Mode I crack propagation even with a unidirectional (along the longitudinal specimen direction) traction load (Fig. 6) and has the following geometric dimensions and mechanical properties:

- width $W=70$ mm, length $L=300$ mm, thickness $t=2.8$ mm, main hole diameter $D=10$ mm, smaller hole diameter $d=5$ mm;
- Young modulus $E=72$ GPa, Poisson coefficient $\nu=0.3$.

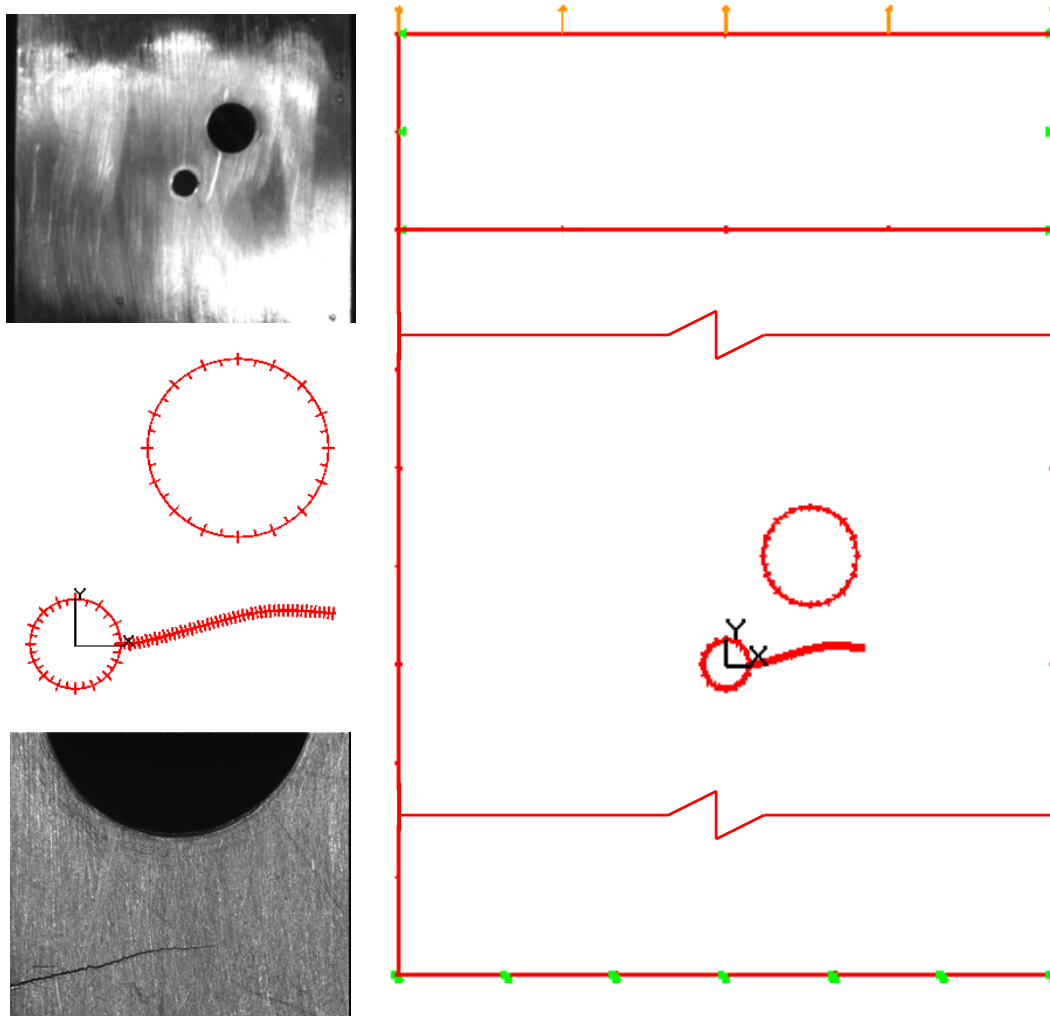


Figure 6. Test specimen and DBEM numerical model: crack path comparison for a propagation under mixed mode conditions.

From the smaller hole a notch of 0.5 mm was cut in order to predetermine the initiation site and, after initiation, the experimental propagation times were monitored. From Fig. 6 it is clearly visible the satisfactory agreement between the numerical and experimental crack propagation path.

An important aspect to be highlighted is the following: few sparse overload cycles intermingled in the baseline load cycles do not modify the crack propagation path with respect to the crack path obtained under constant amplitude conditions, whilst only the crack growth rates are affected. This is very important for the FEM-BEM methodology we have set up because enables the following approach:

- 1) by a DBEM linear elastic crack propagation analysis it is possible to devise the crack path without taking into account the plastic effects coming from load cycle amplitude variation (Fig. 6);
- 2) then the residual stresses along such predetermined crack path are provided by an elastic-plastic FEM analysis, applied to the crack configuration existing at the moment in which the load variation is applied;
- 3) such residual stresses are exported to the DBEM code adopted (BEASY) on the crack configuration reached immediately before the load variation is applied (Fig. 7) and are modeled by line forces (a kind of body loads) along two parallel “load lines” that have a very low offset from the crack axis (a satisfactory accuracy can be obtained keeping such distance inferior than 0.05 mm);
- 4) a DBEM crack propagation analysis is performed with a combined load obtained by the superposition of the residual stresses with the remote load and this time the real crack growth rates are obtained.

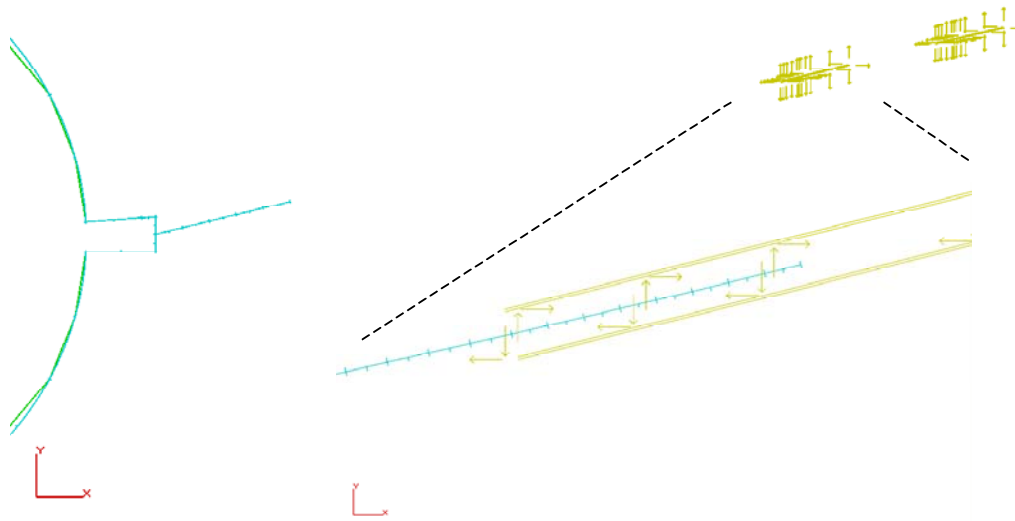


Fig. 7. BEM model with highlight of the superimposed residual stresses.

With reference to the propagation times some non negligible discrepancies are present (Fig. 8), but, considering the inherent scatter and the 2d approximation they can be considered acceptable at this preliminary stage of the research. With reference to the latter it is possible to point out that the crack is experimentally monitored on the surface, where the plastic zone reaches the maximum dimension and consequently the retardation is highest, but the numerical results are related to an average behavior of the crack front along the thickness.

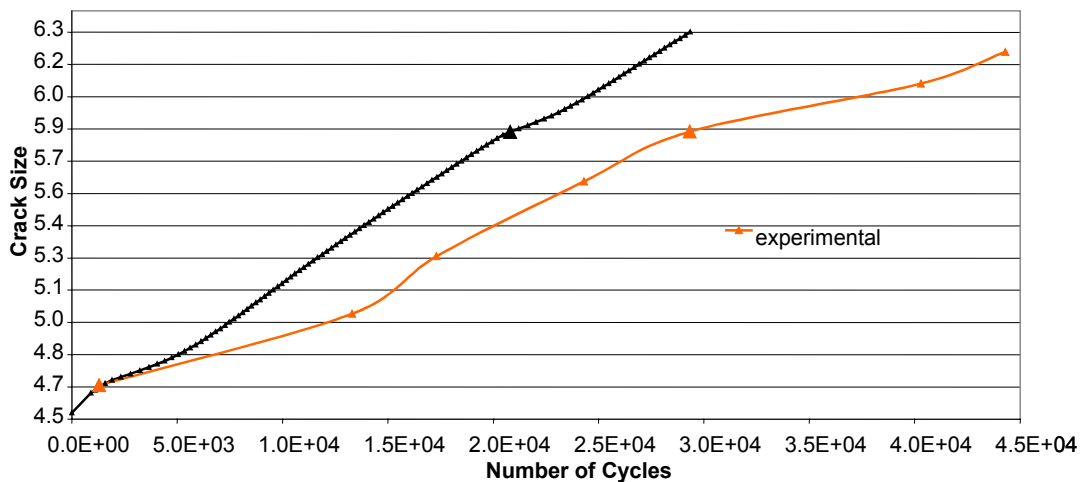


Figure 8. Total number of cycles vs. crack size: numerical and experimental results.

CONCLUSIONS

The procedure described takes advantage of the best capabilities of the two numerical methods (FEM and BEM) and can be easily automated, but most of all it does not require calibration tests because based on a physical description of the crack propagation phenomena under complex load spectrum. The differences between the calculated and experimental delay cycles are comparable with the inherent scatter and, even when the crack path is not known in advance, it is possible to successfully apply this procedure. Further tests are needed but the first outcomes are judged encouraging.

REFERENCES

1. Sadananda K., Vasudevan A.K., (1997), Short crack growth and internal stresses, *International Journal of Fatigue* 19, Supp. No. 1, pp. S99–S108.
2. Sadananda K., Vasudevan A.K., Holtz R.L., Lee E.U., (1999), Analysis of overload effects and related phenomena, *International Journal of Fatigue* Vol. 21, pp. S233–S246.
3. Apicella A., Citarella R., Cricri G., (2006), *Fatigue & Fracture of Engineering Materials & Structures*, (submitted).
4. Cali C., Citarella R., Perrella M., (2003), In: *ESIS STP book Biaxial/Multiaxial Fatigue and Fracture*, pp. 341-360, Carpinteri A., De Freitas M., Spagnoli A. (Ed.), Elsevier.
5. Kim J.K., Shim D.D., (2003), A statistical approach for predicting the crack retardation due to a single tensile overload, *International Journal of Fatigue* 25, pp. 335-342.
6. Cali C., Citarella R., Lepore M., Perrella M., (2005), Integrated system for monitoring the initiation and propagation of fatigue cracks, Conference proceedings “Advances in fracture and damage mechanics IV”, Mallorca, Spain.